

Simulations of Massive Black Hole Binary Mergers

Dale Choi

NASA Goddard Space Flight Center

Greenbelt, MD, USA

In collaboration with

J. Centrella, J. Baker, J. van Meter (NASA/GSFC), M. Koppitz (AEI), & M. C. Miller (UMD)

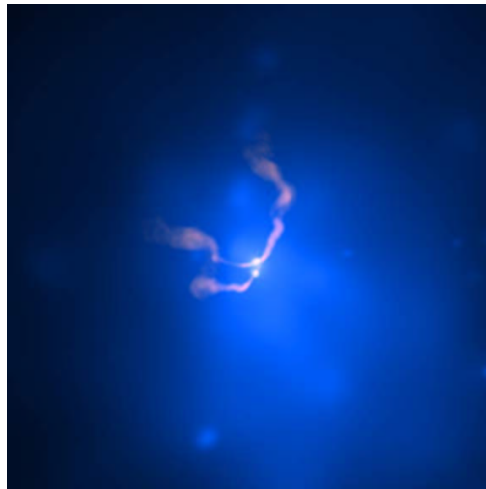
MG11 Meeting, Berlin, Germany, JUL 23–29, 2006

Outline

- Introduction
- Methods
- Results and analysis

Introduction

- Black holes and gravitational waves are among the key predictions of general relativity.
- Super-Massive black holes are believed to be central engines of most active galactic nuclei and play significant roles in formation and evolution of galaxies and various dynamical phenomena such as jets.
- Following galactic merger, a binary black hole system will be formed that can eventually merge into a single black hole emitting gravitational waves.



Composite X-ray(blue) and Radio (pink) image of Abell 400 galaxy cluster

Introduction

- Gravitational waves (GWs) can “probe” deep into the source regions and convey direct information about source dynamics and spacetime geometry for which electromagnetic signals are in general not available.
- Black hole binary systems are among the most anticipated sources of gravitational wave observatories (stellar mass BHs for LIGO/VIRGO/GEO and massive BHs for LISA).
- One of the motivations for simulations of Binary black hole (BBH) mergers is to provide theoretical models/templates for the GW signal.
 - LIGO: S/N for detection of signals can be greatly improved with accurate templates.
 - LISA: Errors in extraction of source parameters and tests of strong-field GR can be reduced with the more accurate modeling of waveforms.
- Understanding of early inspiral phase and late ringdown phase of BBH coalescence are mostly under control. However, understanding of “merger” phase requires numerical relativity simulations, and is an active area of current research.

Methods

- $ds^2 = -\alpha^2 dt^2 + \gamma_{ij}(dx^i + \beta^i dt)(dx^j + \beta^j dt)$
- A version of BSSN system of equations with variables $\{\tilde{\gamma}_{ij}, \phi, \tilde{A}_{ij}, K, \tilde{\Gamma}^i\}$ defined from the usual ADM variables $\{\gamma_{ij}, K_{ij}\}$.

$$\begin{aligned}\phi &= \frac{1}{12} \log \gamma \\ K &= \gamma^{ab} K_{ab} \\ \tilde{\gamma}_{ij} &= e^{-4\phi} \gamma_{ij} \\ \tilde{A}_{ij} &= e^{-4\phi} \left(K_{ij} - \frac{1}{3} \gamma_{ij} K \right) \\ \tilde{\Gamma}^i &= \tilde{\gamma}^{ab} \tilde{\Gamma}_{ab}^i\end{aligned}$$

where $\tilde{\Gamma}_{ab}^i$ Christoffel symbol associated with the conformal metric $\tilde{\gamma}_{ij}$.

- $\{\tilde{\gamma}_{ij} \equiv \tilde{\gamma}_{ij}(t, x, y, z), \phi \equiv \phi(t, x, y, z), \tilde{A}_{ij} \equiv \tilde{A}_{ij}(t, x, y, z), K \equiv K(t, x, y, z), \tilde{\Gamma}^i \equiv \tilde{\Gamma}^i(t, x, y, z)\}$

Methods

- Equation of motion for $\{\tilde{\gamma}_{ij}, \phi, \tilde{A}_{ij}, K, \tilde{\Gamma}^i\}$

$$\begin{aligned}
 \frac{d\phi}{dt} &= -\frac{1}{6}\alpha K \\
 \frac{dK}{dt} &= -\nabla^a \nabla_a \alpha + \alpha \left(\tilde{A}_{ab} \tilde{A}^{ab} + \frac{1}{3} K^2 \right) \\
 \frac{d\tilde{\gamma}_{ij}}{dt} &= -2\alpha \tilde{A}_{ij} \\
 \frac{d\tilde{A}_{ij}}{dt} &= e^{-4\phi} (-\nabla_i \nabla_j \alpha + \alpha R_{ij})^{\text{TF}} + \alpha \left(K \tilde{A}_{ij} - 2\tilde{A}_{ia} \tilde{A}^a_j \right) \\
 \frac{\partial \tilde{\Gamma}^i}{\partial t} &= 2\alpha \left(\tilde{\Gamma}^i_{ab} \tilde{A}^{ab} - \frac{2}{3} \tilde{\gamma}^{ia} K_{,a} + 6\tilde{A}^{ia} \phi_{,a} \right) \\
 &\quad - \tilde{\Gamma}^j \beta^i_{,j} + \frac{2}{3} \tilde{\Gamma}^i \beta^j_{,j} + \beta^k \tilde{\Gamma}^i_{,k} \\
 &\quad + \tilde{\gamma}^{jk} \beta^i_{,jk} + \frac{1}{3} \tilde{\gamma}^{ij} \beta^k_{,kj} - 2\tilde{A}^{ia} \alpha_{,a} - \left(\chi_{yo} + \frac{2}{3} \right) \left(\tilde{\Gamma}^i - \tilde{\gamma}^{kl} \tilde{\Gamma}^i_{kl} \right) \beta^m_{,m}
 \end{aligned}$$

where $d/dt = \partial/\partial t - \mathcal{L}_\beta$. The last term in $\tilde{\Gamma}^i$ equation suggested by Yo et al to suppress exponential growth of $\tilde{\Gamma}^i$ when $\beta^j_{,j} > 0$.

Methods

- Constraint equations are solved only at $t = 0$ to set up initial data.
- Initial data: Assume conformal flatness and maximal slicing ($\tilde{\gamma}_{ij} = \eta_{ij}, K = 0$)
- Take Bowen York form of extrinsic curvature

$$K^{ij} = \frac{3}{2r^2}(P^i n^j + P^j n^i - (\gamma^{ij} - n^i n^j)P^k n_k) + \frac{3}{r^3}(\epsilon^{ikl} S_k n_l n^j + \epsilon^{jkl} S_k n_l n^i)$$

- Puncture method: split $\phi = \phi_{BL} + u$, $\phi_{BL} = 1 + \sum_{n=1}^2 \frac{m_n}{2|\vec{r} - \vec{r}_n|}$ where the n^{th} black hole has mass (parameter) m_n and is located at coordinate \vec{r}_n . We solve HCE for u using MultiGrid algorithm.

$$\Delta u + \beta \left(1 + \frac{u}{\phi_{BL}}\right)^{-7} = 0, \beta = \frac{1}{8} \phi_{BL}^{-7} K^{ij} K_{ij}$$

- For $t > 0$, we directly finite-difference the whole ϕ w/o making the split. May generate non-convergence or lower-order convergence near “punctures”. In practice, puncture “errors” do not influence the dynamics outside the horizon. Combined with proper choices of gauges, this strategy is proven to be a robust way to realize moving black hole idea without a need for excision technique. (Hannam et al, 2006)

Methods

- Gauge conditions do NOT change dynamics, but turn out to be crucial in getting stable numerical evolution.
- Gauge conditions: specify α, β^i . We currently use the following conditions (van Meter, Baker, Koppitz, Choi, PRD, 2006)

$$\begin{aligned}\partial_t \alpha &= -2\alpha K + \beta^i \partial_i \alpha \\ \partial_t \beta^i &= \frac{3}{4} B^i + \beta^j \partial_j \beta^i \\ \partial_t B^i &= \partial_t \tilde{\Gamma}^i - \beta^j \partial_j (\tilde{\Gamma}^j - B^i) - \eta B^i\end{aligned}$$

where η is a constant typically between (1, 2).

Waveform Analysis

- Use NP Weyl tensor component Ψ_4 to analyse (outgoing) gravitational wave content.
- Harmonic decomposition

$$\Psi_4(r, \theta, \phi, t) = \sum_{lm} A_{lm}(r, t) {}_{-2}Y_{lm}(\theta, \phi)$$

$$A_{lm}(r, t) = \int \Psi_4(r, \theta, \phi, t) {}_{-2}Y_{lm}(\theta, \phi) d\Omega$$

- Given Ψ_4 , one can calculate E, J_z, P_z .

$$E = \frac{r^2}{4\pi} \int \int_{\Omega} \left| \int_{-\infty}^t dt' \Psi_4(t', r, \theta, \phi) \right|^2 d\Omega dt$$

$$P_z = \frac{r^2}{4\pi} \int \int_{\Omega} \cos \theta \left| \int_{-\infty}^t dt' \Psi_4(t', r, \theta, \phi) \right|^2 d\Omega dt$$

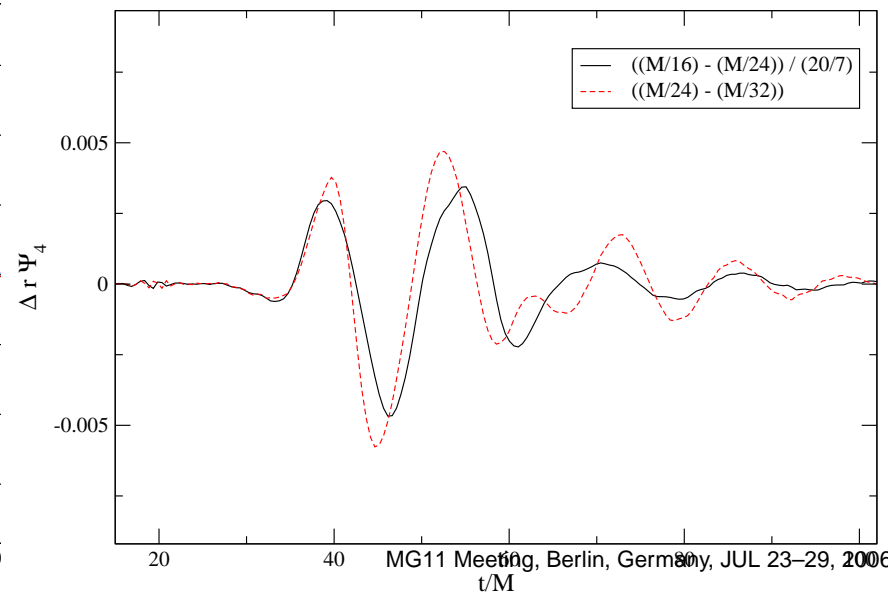
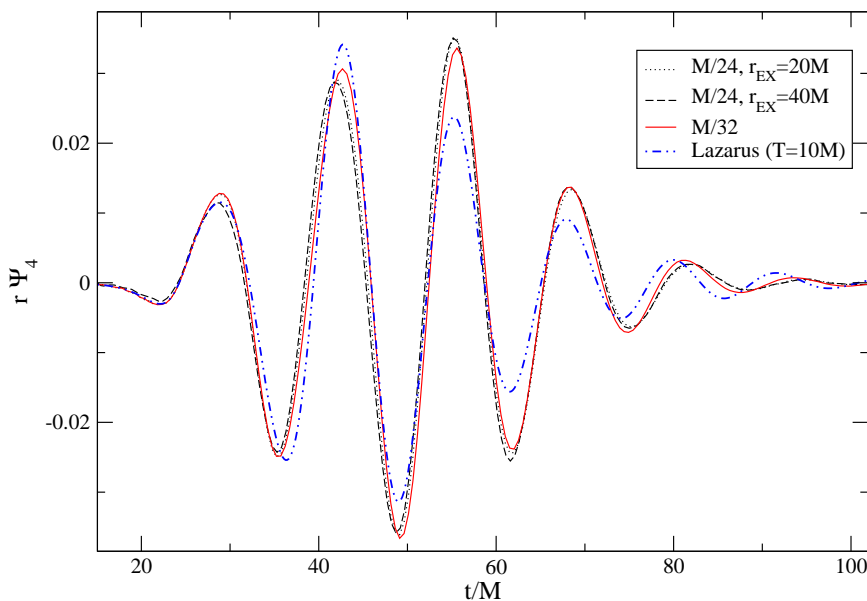
$$J_z = -\frac{r^2}{4\pi} \int \operatorname{Re} \left[\int_{\Omega} d\Omega (\partial_{\phi} \int_{-\infty}^t dt' \psi_4(t', r, \theta, \phi)) \right. \\ \left. \times \left(\int dt' \int d\tilde{t} \bar{\psi}_4(\tilde{t}, r, \theta, \phi) \right) \right] dt$$

Some numerical details

- Initial Data: MultiGrid algorithm.
- Evolution: Finite difference method
 - Spatial differencing: 4th order (centered/upwind)
 - Time integration: iterative Crank Nicholson / RK4 time integrator.
- Outer Boundary: causally disconnected from the region of spacetime of interests. Simple out-going wave boundary conditions are used. Typical computational domain: $[-256M, 256M] \times [-256M, 256M] \times [0M, 256M]$ or larger depending on total simulation time.
- Use PARAMESH package to implement parallelism and adaptivity.
- Scaling performance is good $\sim 86(67)\%$ level up to 1016(2032) CPUs for the full AMR simultaions.

Results: Inspiral $L/M \sim 4.99$ “QC0”

- Baker, Centrella, Choi, Koppitz, van Meter, Phys. Rev. Lett. **96**, 111102 (2006)
- Initial data based on Cook (1994): $L/M = 4.99$, $J/M^2 = 0.779$ with M total (initial) ADM mass.
- Grid set-up: FMR with MR boundaries located at $2M, 4M, 8M, 16M, 32M, 64M$ with OB at $128M$
- Resolutions run: $h_f = M/16, M/24, M/32$
- Confirmed solution convergence and waveform convergence



Results: Inspirals with larger L/M

- Baker, Centrella, Choi, Koppitz, van Meter, Phys. Rev. **D73**, 104002 (2006)
- Consider initial data with a larger separation than “QC0”.
- $L/M = 9.9, 11.1, 12.1, 13.2$ (Runs: R1, R2, R3, R4)
- Grid set-up
 - Initially grids are set-up by hand (FMR)
 - During the evolution, adaptive mesh refinement based on a function called the real part of Coulomb scalar χ . In terms of the curvature invariants I , J , and S ,

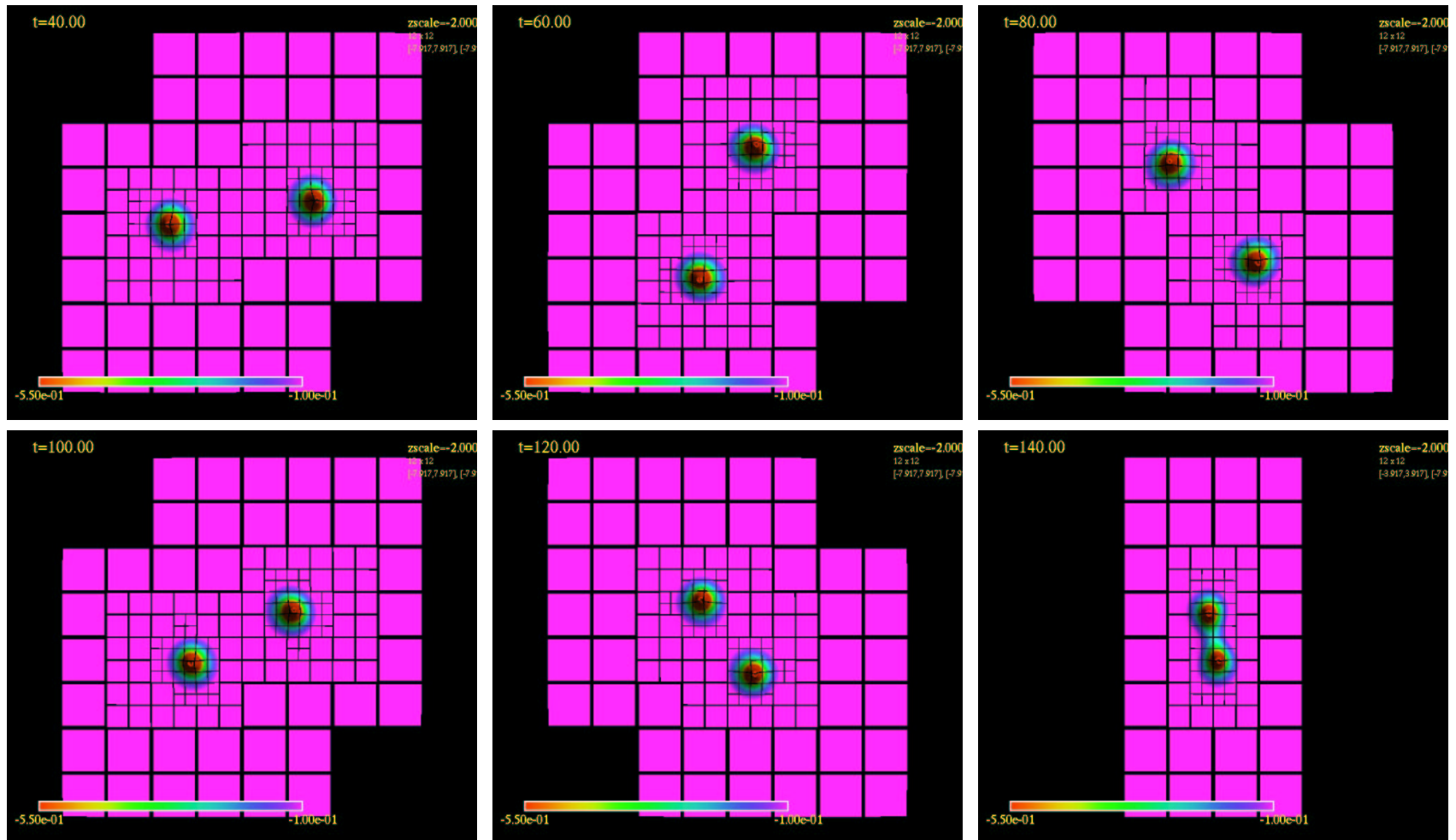
$$\chi = -\frac{3J \left(W^{\frac{1}{3}} + W^{-\frac{1}{3}} \right)}{2I\sqrt{S}}$$
$$W \equiv \sqrt{S} - \sqrt{S-1}$$

Results: R1–R4

- Question I: can we separate initial time transient part of the waveforms from the actual merger waveforms?
- Answer I: agreement between waveforms from runs with different initial separation indicate that initial data transients go away during the first orbit or so. Turns out initial separation for QC0 run was too small.
- Question II: what is the dependence of waveforms on the initial data with increasing separation? are there any features in the actual merger waveforms?
- Answer II: Remarkable agreement for the last orbit, merger and ringdown for all 4 runs (R1–R4). There seems to be universal features. All the memory about the initial data seems to be washed away.

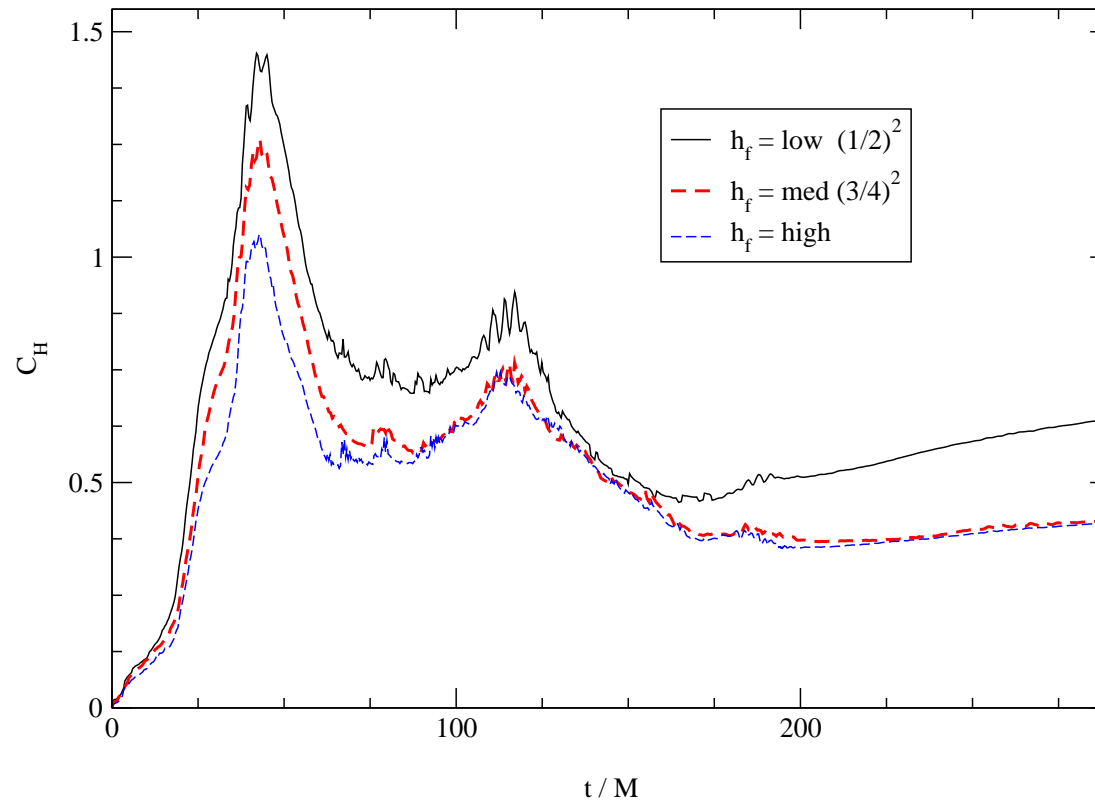
Results: Solution R1

- Snapshots of grid structure: $\text{Re}(\chi)$ on $z = 0$ plane at $t = 40M, 60M, 80M, 100M, 120M, 140M$ [MOVIE 1]



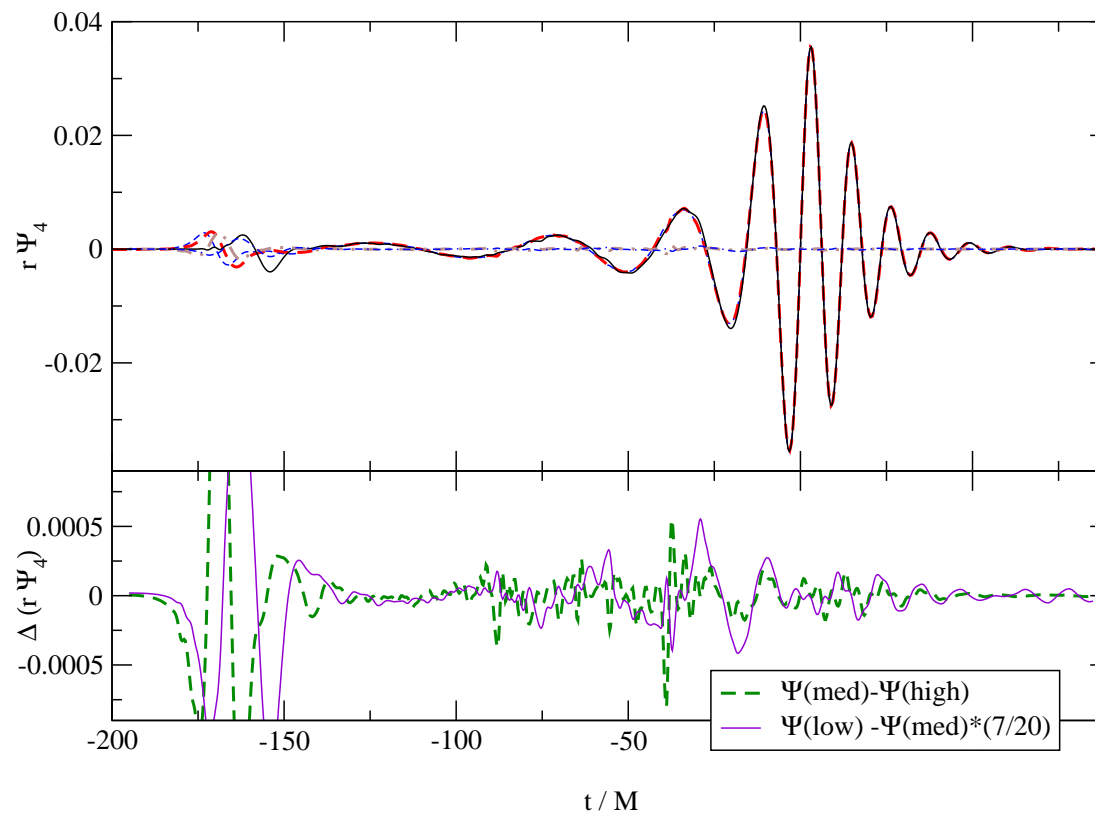
Results: R1 HC errors

- R1 runs: Hamiltonian Constraint errors. Resolutions: $h_f = 3M/64, M/32, 3M/128$.



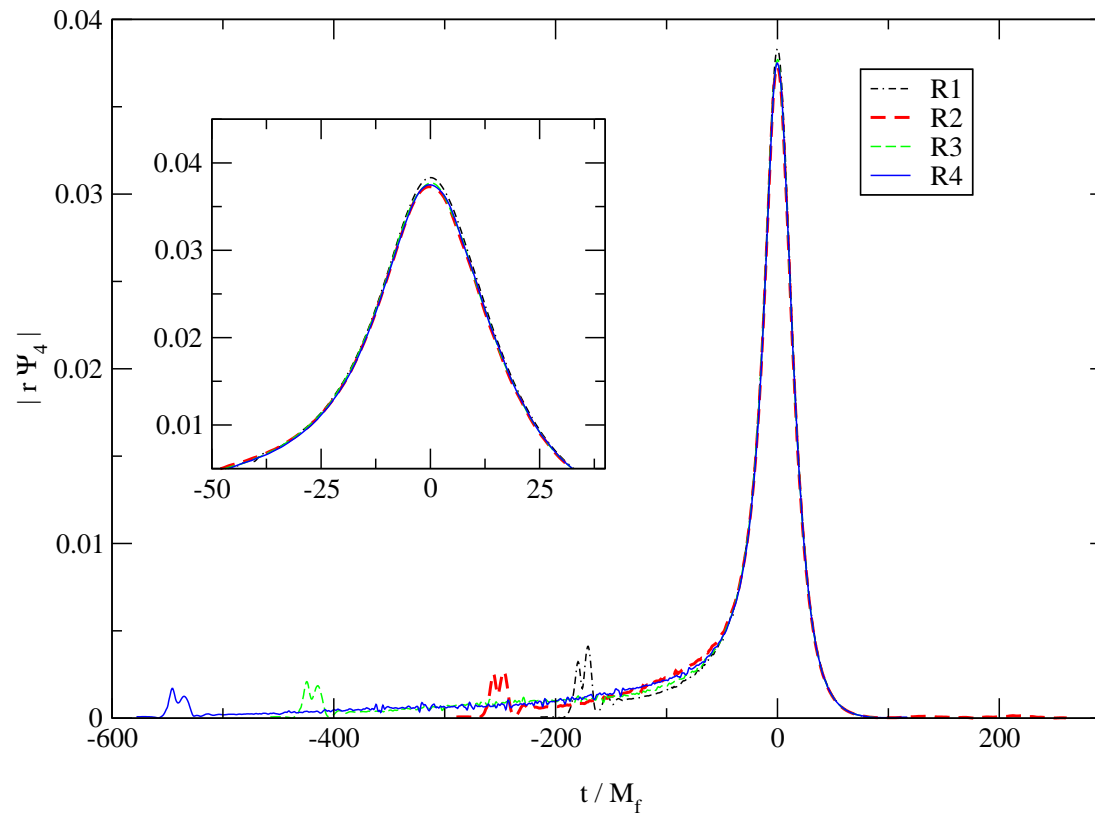
Results: Gravitational Waveforms

- R4 run: [MOVIE 2]
- R1 runs: Errors in Gravitational Waveforms ($h_f = 3M/64, M/32, 3M/128$)



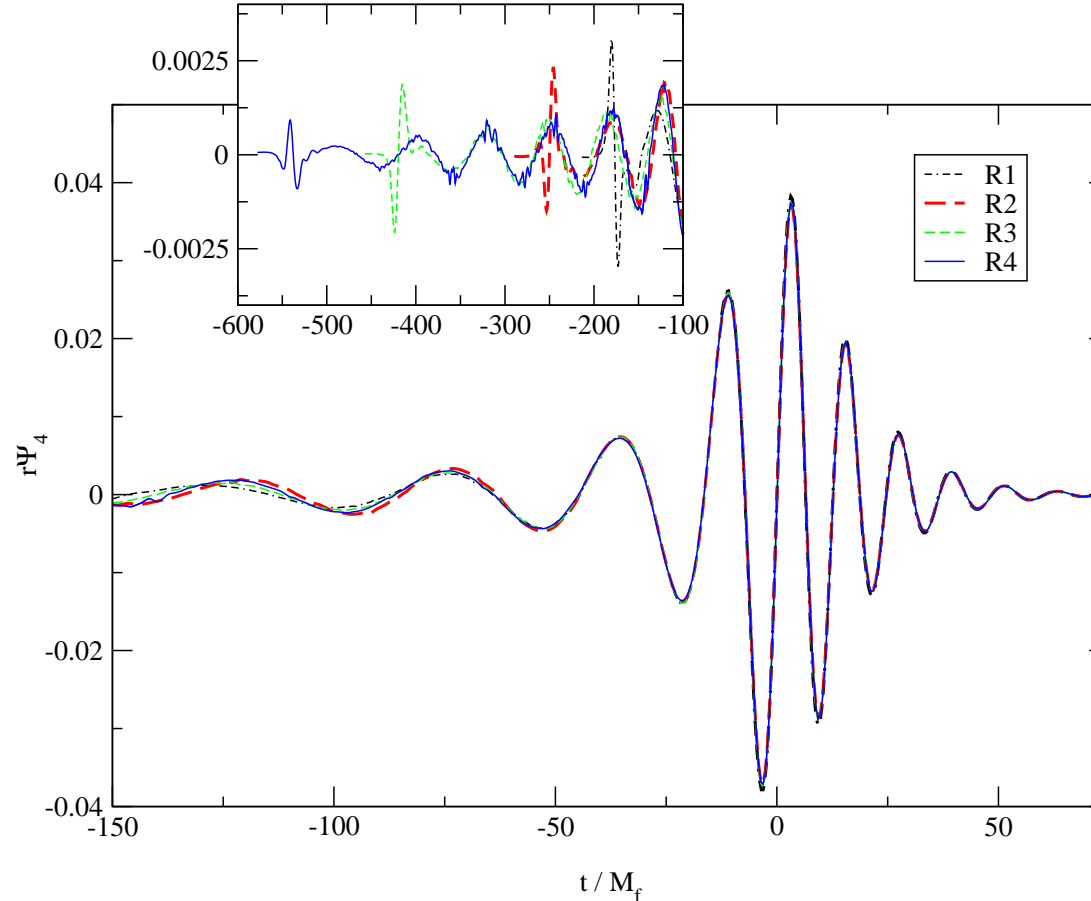
Results: Wave amplitude from R1–R4

- $r\Psi_4(t) = A(t)\exp(-i\varphi(t))$
- Waveform amplitude, $A(t)$. (Time-shifted to match the maximum amplitude.)



Results: Waveforms from R1–R4

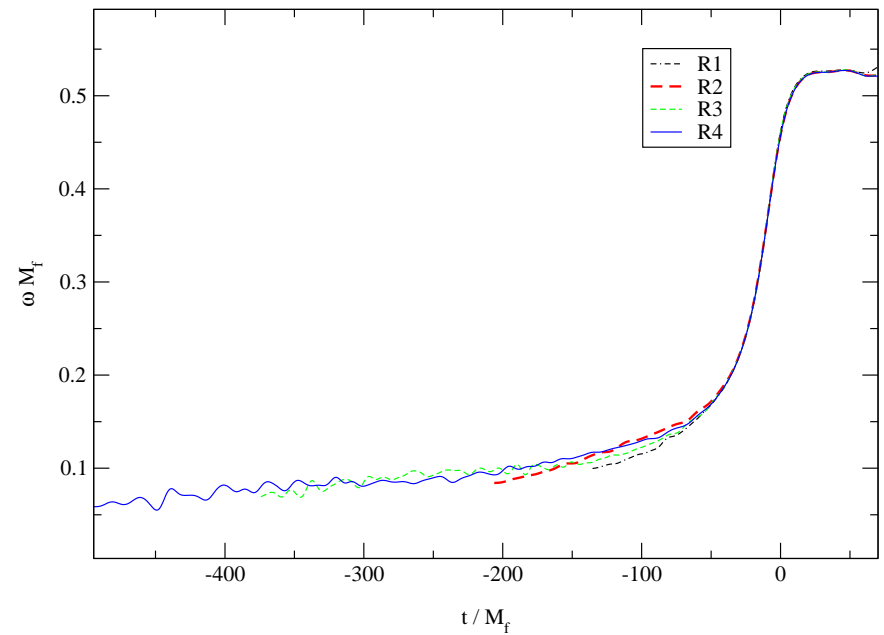
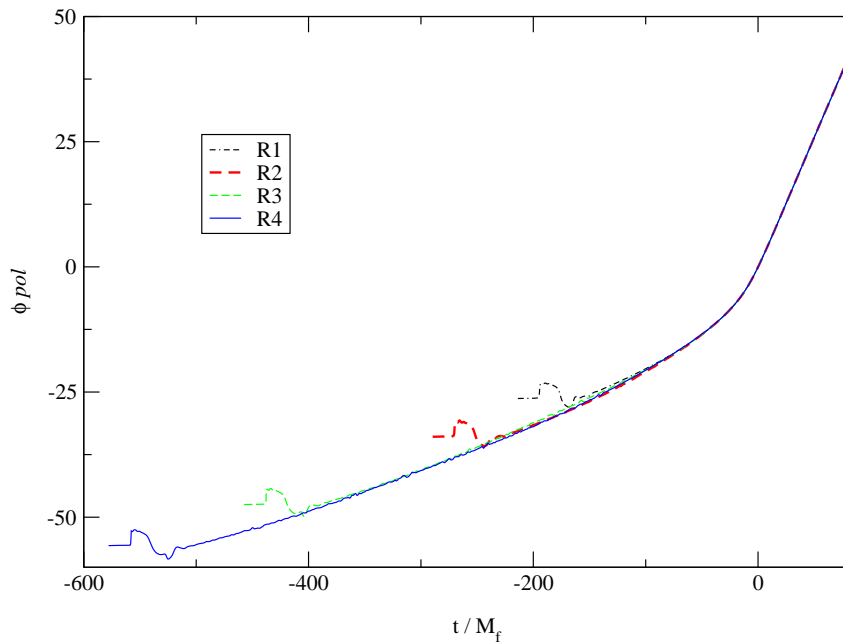
- $r\Psi_4(t)$: $L = 2, M = 2$ (the dominant mode).
- Excellent agreement among the runs for $t > -50M_f$ at $\sim 1\%$ level and errors are within 10% level prior to that.



Results: Pol. Angle & Wave Freq.

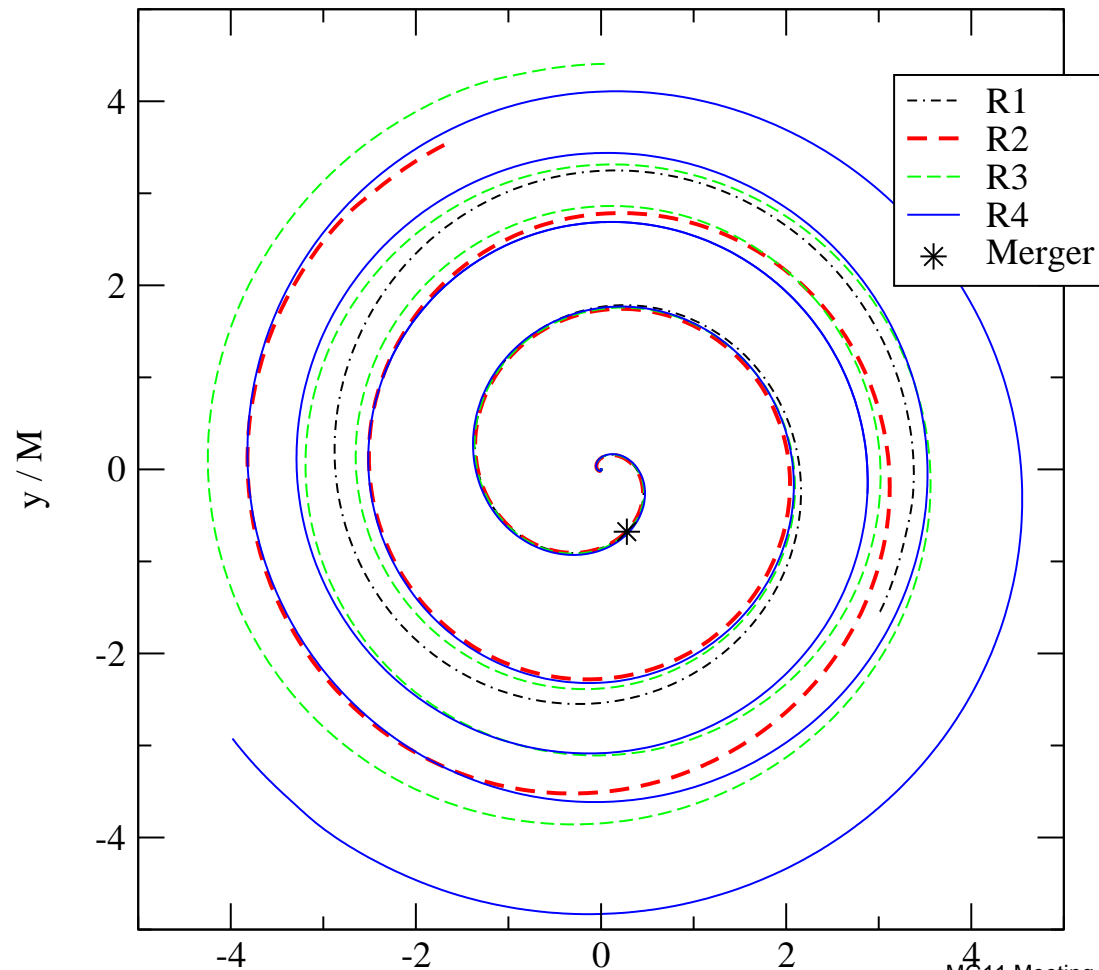
● Polarization angle, $\varphi(t)$ ($r\Psi_4(t) = A(t)\exp(-i\varphi(t))$)

● Wave frequency $\omega = \partial\varphi(t)/\partial t$ ($M_{sun} \sim 5\mu s$)



Results: Puncture tracks from R1–R4

● “Puncture” trajectories: $\dot{\vec{x}}_{punc} = -\vec{\beta}(\vec{x}_{punc})$



Results: E, J from R1–R4

- Energy and angular momenta for the radiation and final black hole. E_{rad} and J_{rad} are measured at $r_{ex} = 30M$, and $r_{ex} = 50M$, respectively. M_{QN} and a_{QN} are calculated independently from the quasi-normal fits of the ringdown waveforms, and agree well with the values deduced from the radiative losses.

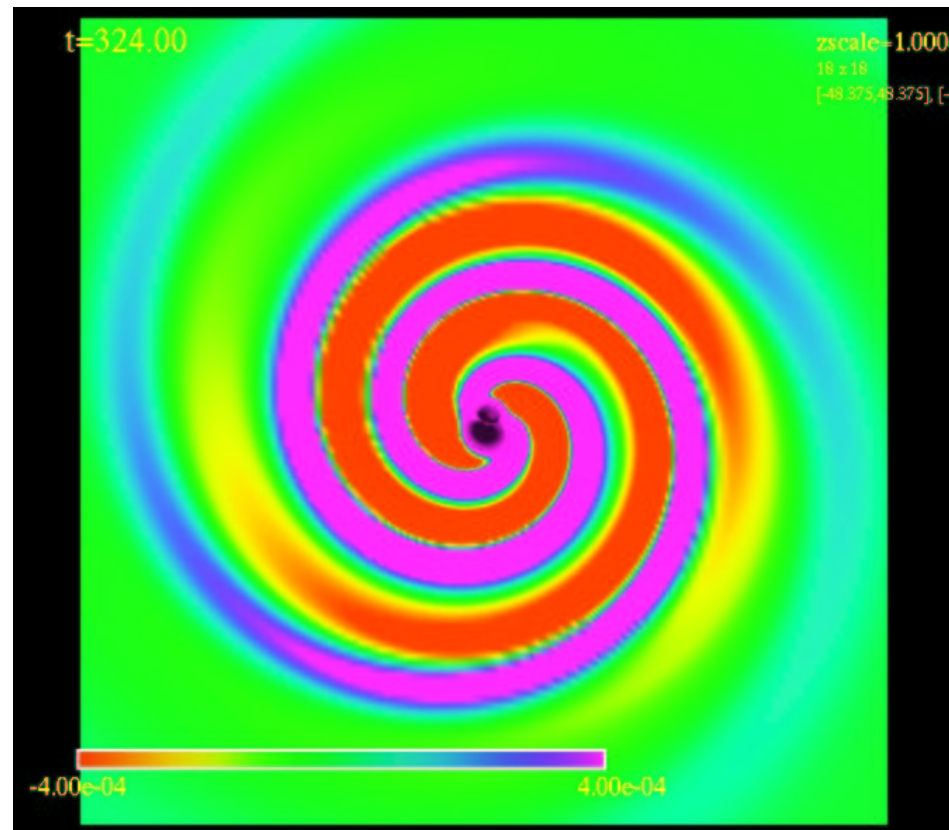
	E_{rad}/M_f	J_{rad}/M_f^2	a/M_f	M_{QN}/M_f	a_{QN}/M_f
$R1$	0.036	0.25	0.69	1.005	0.72
$R2$	0.037	0.27	0.69	1.002	0.69
$R3$	0.038	0.31	0.69	1.004	0.69
$R4$	0.039	0.33	0.70	1.004	0.69

Results: Non-equal mass collision

- Motivation: asymmetric emission of GWs can impart astrophysical kick to the merger remnant.
- Large kick velocity can unbound the merged black hole from the center of the host structure → astrophysically very interesting value.
- Recent numerical calculations by Campanelli (2005) & PSU group (2006).
- Start with a simple case: mass ratio $\rho = M_1/M_2 = 2/3 (= 0.667)$.
- Mode analysis indicate that dominant contribution comes from $L = 2, M = 2$ and $L = 3, M = 3$ mixing.

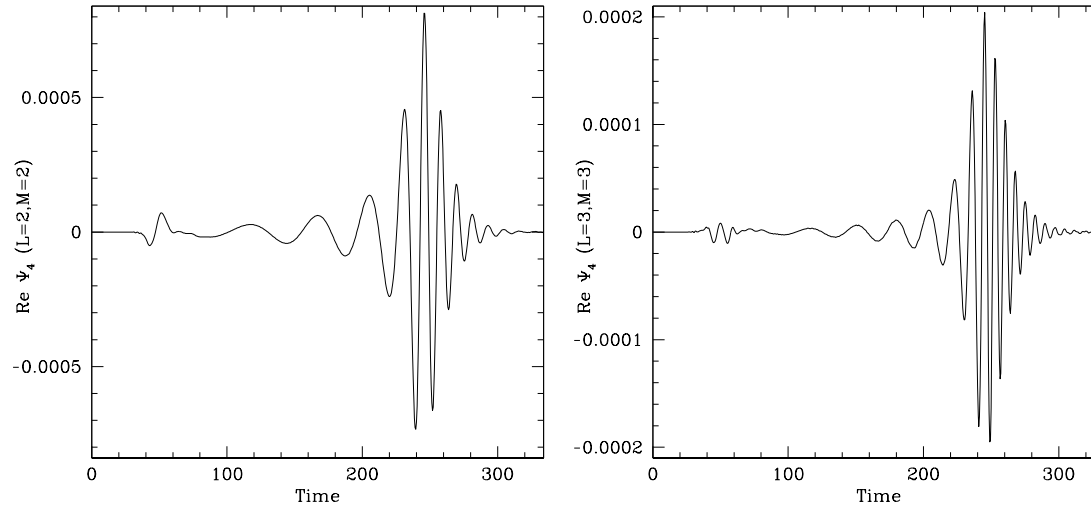
Results: Non-equal mass collision, Ψ_4

- Initial separation $\sim 9M$, $h_f = M/21.3$
- $\Psi_4(t, x, y, z = 0)$ (real part) on $Z = 0$ plane [MOVIE 3]
- Ψ_4 still dominated by $L = 2, M = 2$ mode and asymmetry is a very subtle effect.



Results: Non-equal mass collision: Kicks

- Waveforms at $r_{ext} = 30M$: $L = 2, M = 2$ part and $L = 3, M = 3$ part.



- $\omega_{22}/\omega_{33} \sim 2/3$.
- Simulations with three different initial separation (coord separation of $4.1M, 6.2M, 7.1M$) are used to analyze the final kick. ($h_f = M/32, M/40, M/48$)
- “kick” = $v(t) = \frac{1}{M} \sqrt{\left(\int^t \frac{dP_x(t')}{dt'} dt'\right)^2 + \left(\int^t \frac{dP_y(t')}{dt'} dt'\right)^2}$
- Kick velocity $\sim 105(\pm 10)$ km/s from the last orbit for $\rho = M_1/M_2 = 2/3$.

Concluding Remarks

- Our gravitational waveform and trajectory analysis provide a consistent picture.
- Results for equal mass non-spinning binaries indicate that gravitational waveforms have universal features for the last orbit, merger, and ring-down.
- Early simulations to calculate gravitational radiation recoil kick are underway.
- Future: large parameter space still to be explored (e.g. different mass ratio, spin, etc).